AGU PUBLICATIONS

Geophysical Research Letters

RESEARCH LETTER
10.1002/2014GL059940

Key Points:
- Labrador Sea ice edge is not the sole determinant of the surface heat fluxes
- Topographic flow distortion is also vital to air-sea interaction
- Observed oceanic convection is coincident with surface heat flux maximum

Correspondence to:
G. W. K. Moore,
gwk.moore@utoronto.ca

Citation:
Moore, G. W. K., R. S. Pickart, I. A. Renfrew, and K. Våge (2014), What causes the location of the air-sea turbulent heat flux maximum over the Labrador Sea?, *Geophys. Res. Lett.*, *41*, 3628–3635, doi:10.1002/2014GL059940.

Received 18 MAR 2014
Accepted 24 APR 2014
Accepted article online 29 APR 2014
Published online 19 MAY 2014

What causes the location of the air-sea turbulent heat flux maximum over the Labrador Sea?

G.W.K. Moore[1], R.S. Pickart[2], I.A. Renfrew[3], and Kjetil Våge[4]

[1]Department of Physics, University of Toronto, Toronto, Ontario, Canada, [2]Department of Physical Oceanography, Woods Hole Oceanographic Institution, Woods Hole, Massachusetts, USA, [3]Centre for Ocean and Atmospheric Sciences, School of Environmental Sciences, University of East Anglia, Norwich, UK, [4]Geophysical Institute, University of Bergen and Bjerknes Centre for Climate Research, Bergen, Norway

Abstract The Labrador Sea is a region of climatic importance as a result of the occurrence of oceanic wintertime convection, a process that is integral to the Atlantic Meridional Overturning Circulation. This process requires large air-sea heat fluxes that result in a loss of surface buoyancy, triggering convective overturning of the water column. The Labrador Sea wintertime turbulent heat flux maximum is situated downstream of the ice edge, a location previously thought to be causal. Here we show that there is considerable similarity in the characteristics of the regional mean atmospheric circulation and high heat flux events over the Labrador Sea during early winter, when the ice is situated to the north, and midwinter, when it is near the region of maximum heat loss. This suggests that other factors, including the topography of the nearby upstream and downstream landmasses, contribute to the location of the heat flux maximum.

1. Introduction

The Labrador Sea (Figure 1) is one of the few sites in the subpolar North Atlantic Ocean where deep oceanic convection occurs [*Marshall et al.*, 1998; *Marshall and Schott*, 1999; *Pickart et al.*, 2002]. The resultant water mass, known as Labrador Sea Water [*Clarke and Gascard*, 1983], is an important contributor to the lower limb of the Atlantic Meridional Overturning Circulation (AMOC) [*Talley et al.*, 2003]. Climate models tend to predict a weakening of the AMOC, often as a result of a reduction in the formation rate of Labrador Sea Water, as one of the responses to a warming climate [*Stouffer et al.*, 2006; *Rhein et al.*, 2011]; a correspondence that has also recently been suggested by observations [*Robson et al.*, 2014].

Open-ocean convection is facilitated by a preconditioned water column with a reduced stratification, usually the result of an upward doming of isopycnals within a cyclonic gyre, and elevated fluxes of sensible and latent heat from the ocean to the atmosphere [*Marshall et al.*, 1998; *Marshall and Schott*, 1999]. The general circulation of the Labrador Sea consists of a boundary current that encircles the basin, with an extended region of cyclonic flow offshore [*Lavender et al.*, 2002]. The preconditioning of the water column is aided by the accumulated buoyancy loss throughout the cool period of the year that acts to erode any remaining stratification in the mixed layer. As such, high heat flux events in middle to late winter can trigger the convective overturning, sometimes to depths exceeding 1500 m [*Clarke and Gascard*, 1983; *Pickart et al.*, 2002].

The Labrador Sea experiences a number of cold air outbreaks each winter when the northwesterly flow behind a passing synoptic-scale or mesoscale cyclone advects cold, dry air off the continent over the relatively warm surface waters, resulting in elevated total turbulent heat fluxes often in excess of 600 W/m^2 [*Renfrew and Moore*, 1999; *Renfrew et al.*, 2002; *Sathiyamoorthy and Moore*, 2002; *Kolstad et al.*, 2009]. It is thought that these events are the triggers for the initiation of the overturning of the water column [*Marshall et al.*, 1998; *Marshall and Schott*, 1999], and most of the research on the atmospheric forcing of oceanic convection in the Labrador Sea has focused on these trigger events [*Marshall et al.*, 1998; *Renfrew and Moore*, 1999; *Renfrew et al.*, 1999; *Pagowski and Moore*, 2001; *Myers and Donnelly*, 2008; *Våge et al.*, 2009a]. During this period, sea ice is typically located just upstream of the convective region and it has been assumed that the proximity of the ice plays an important role in the spatial pattern of the heat fluxes [*Brummer*, 1996; *Marshall and Schott*, 1999; *Olsson and Harrington*, 2000; *Pagowski and Moore*, 2001; *Fenty and Heimbach*, 2013]. However, as is shown below, the spatial structure of the air-sea heat fluxes over the Labrador Sea—in the mean and during cold air outbreaks—is surprisingly similar during both the early winter period, when sea ice

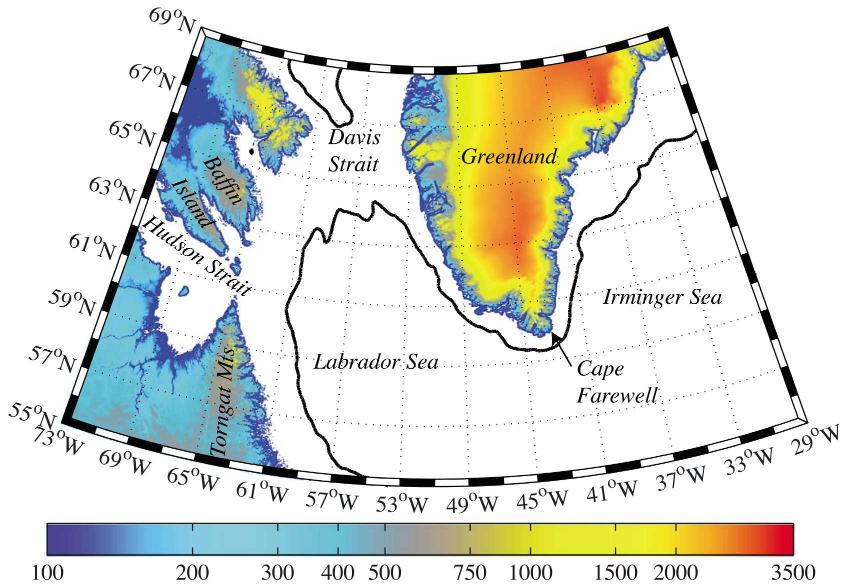

Figure 1. The topography (m) and place names in the region of interest. Also shown by the thick black line is the 1000 m isobath. The topography and bathymetry data are from the ETOPO1 data set.

is not present in the vicinity of convection, and the midwinter period, when it is. This suggests that proximity to the sea ice edge is not the only factor responsible for the location of the heat flux maximum and that other processes, such as upstream and downstream topographic flow distortion, need to be considered.

2. Data and Methods

Greenland flow distortion typically results in mesoscale atmospheric variability with length scales on the order of 200–400 km [*Moore and Renfrew*, 2005; *Renfrew et al.*, 2008]. Given that the global reanalyses typically have effective horizontal resolutions on the order of 400–500 km [*Condron and Renfrew*, 2013; *Laffineur et al.*, 2014], there is concern that they may not be able to fully resolve details of the flow in the vicinity of Greenland and the associated air-sea interaction. For this reason, we have chosen to use the surface meteorological fields from the North American Regional Reanalysis (NARR) [*Mesinger et al.*, 2006] in this study. The horizontal grid spacing of the NARR is 32 km, and it is estimated that its effective horizontal resolution is on the order of 200 km [*Skamarock*, 2004], allowing for an improved view of the flow in the region. Indeed, studies near Greenland have indicated that NARR surface meteorological fields are in good agreement with both buoy and aircraft observations [*Moore et al.*, 2008; *Renfrew et al.*, 2009]. Here we use the full 3-hourly resolution data for the months of January, February, November, and December 1979–2012.

Although the surface meteorological fields from reanalyses are typically well constrained by observations, the air-sea fluxes may not be because of their strong dependence on surface and boundary layer parameterizations in the underlying numerical model [*Smith et al.*, 2001; *Renfrew et al.*, 2002]. The NARR surface heat fluxes in the coastal waters off Greenland were shown by *Renfrew et al.* [2009] to be biased high compared to other analyses/reanalyses and observations. Accordingly, we have chosen to use a well-established bulk-flux algorithm [*Smith*, 1988; *DeCosmo et al.*, 1996] that has been shown to agree with in situ high-latitude heat flux measurements [*Renfrew et al.*, 2002], with NARR surface fields as input variables to calculate the sensible and latent heat fluxes. The sign convention used is that fluxes out of the ocean are positive.

Data from Argo floats that sampled the upper ocean in the Labrador Sea from February to April during 2000–2007 are used to identify where oceanic convection tends to occur [*Våge et al.*, 2009a]. The maximum late winter mean mixed-layer depth in the Labrador Sea from this data was 950 m, and, for the purposes of this paper, the 700 m mixed-layer depth contour was used to delineate the region of convection. This area is in general agreement with that determined from hydrographic data during active convection [*Lavender et al.*, 2000; *Pickart et al.*, 2002].

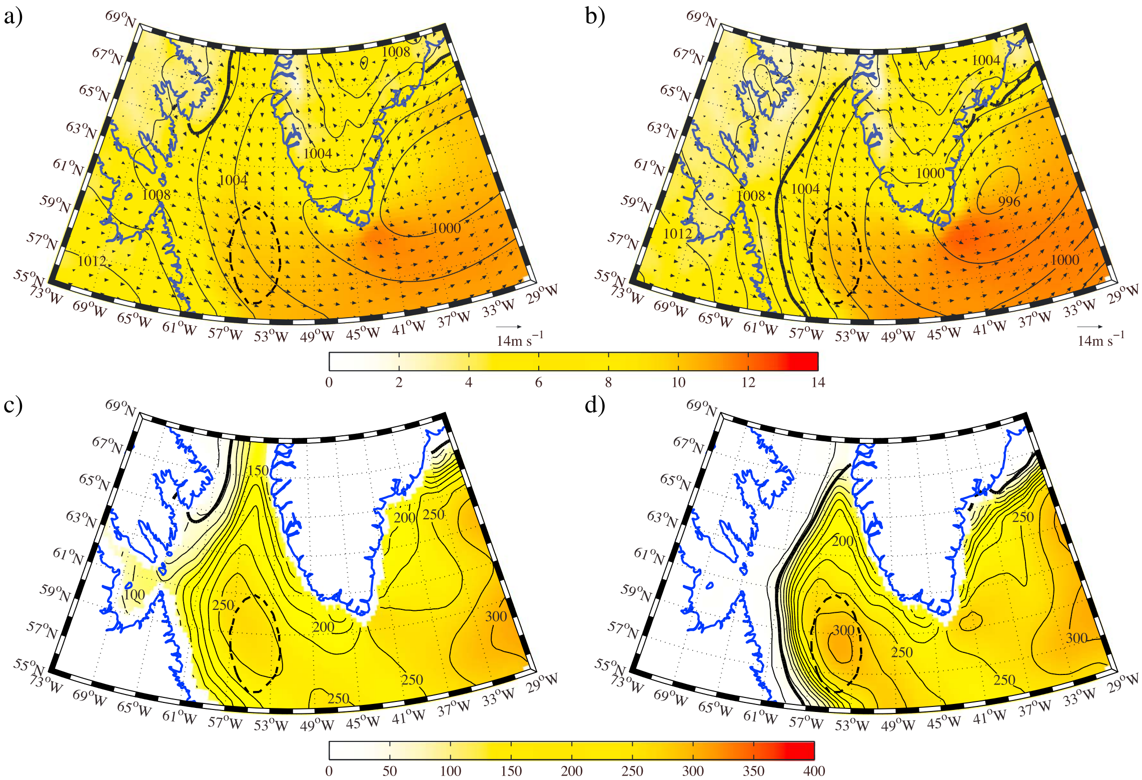

Figure 2. The monthly mean sea level pressure field (contours: mbar), the 10 m wind field (vectors: m s^{-1}), and the 10 m wind speed field (shading: m s^{-1}) during (a) November and December and (b) January and February 1979–2102. The monthly mean total turbulent heat flux field (contours and shading: W m^{-2}) during (c) November and December and (d) January and February 1979–2102. The thick black line indicates the corresponding monthly mean 50% sea ice concentration contour, while the dashed black oval indicates the climatological mean 700 m mixed layer depth.

3. Results

We compare two seasonal time periods in our study: early winter (November and December) and midwinter (January and February). Figure 2 shows the monthly mean fields of sea level pressure, 10 m wind, and total turbulent heat flux (sum of the sensible and latent heat fluxes—henceforth referred to as Q_{THF}) for these two periods. Also shown is the mean 50% sea ice concentration contour as determined using the NASA Team algorithm [*Parkinson and Cavalieri*, 2008]. The region of convection, based on the Argo data, is also indicated. The structure of the various fields during the two periods is remarkably similar with a spatial correlation coefficient over the domain in Figure 2 for each field exceeding 0.9. During both periods, the Labrador Sea is dominated by a northwesterly cyclonic flow associated with the Icelandic Low which is situated to the east of Cape Farewell (Figures 2a and 2b). The asymmetry of the sea level pressure field over the Greenland ice sheet and in its lee over the Irminger Sea is evidence of the flow distortion associated with the high topography of Greenland [*Renfrew et al.*, 2008]. As expected, the Icelandic Low is deeper during the midwinter period (by approximately 4 mbar) compared to the early winter period. However, over the convection site, the mean 10 m wind speeds during the midwinter period are only 3% higher than those during the early winter period. During the early winter period, the sea ice extends only as far south as Baffin Island, while in the midwinter period, it is present all along the Labrador Coast. The monthly mean 10 m wind speeds in the region of Hudson and Davis Straits are 25% higher in the November-December period compared to the January-February period, presumably the result of the increase in surface roughness over the sea ice present in these regions during the latter months [*Liu et al.*, 2006; *Petersen and Renfrew*, 2009].

The Q_{THF} field (Figures 2c and 2d) has a maximum over the Labrador Sea convection region during both periods, with the maximum during the midwinter period exceeding that during the early winter period by 17%. In midwinter, the sea ice along the Labrador and Baffin Island coasts results in a significant increase in the gradient of Q_{THF} to the west of the maximum. Apart from this feature, the overall structure of the Q_{THF}

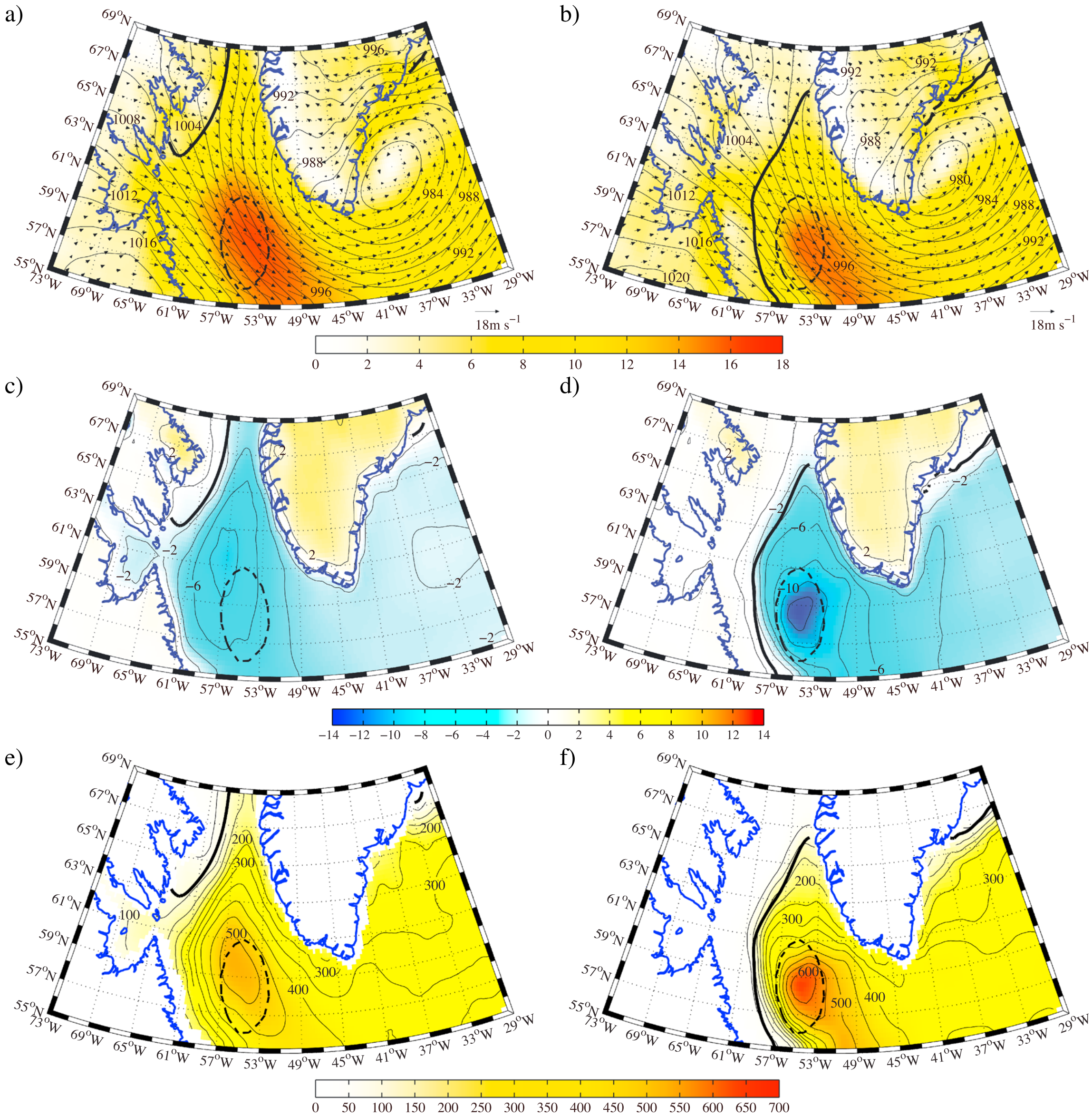

Figure 3. The composite sea level pressure field (contours: mbar), the 10 m wind field (vectors: m s^{-1}), and the 10 m wind speed field (shading: m s^{-1}) for northwesterly wind events that result in total turbulent heat fluxes over the Labrador Sea convection site that exceed the 95th percentile value during (a) November and December and (b) January and February 1979–2012. The composite air-surface temperature difference field (contours and shading: °C) for these events during (c) November and December and (d) January and February 1979–2012. The composite total turbulent heat flux field (contours and shading: W m^{-2}) for these events during (e) November and December and (f) January and February 1979–2012. The thick black lines indicate the corresponding composite 50% sea ice concentration contour, while the dashed black curve indicates the climatological mean 700 m mixed layer depth.

field is similar during both periods, consistent with a spatial correlation coefficient that exceeds 0.9. There is a secondary maximum in Q_{THF} immediately east of Cape Farewell that is associated with westerly tip jets that develop in this region and force oceanic convection in the Irminger Sea [*Pickart et al.*, 2003].

To identify high heat flux events in the Labrador Sea, we employed the following methodology. The 3-hourly NARR data for the period 1979–2012 were used to generate time series of Q_{THF} at the center of the convection region (59°N, 54°W) for both the early and midwinter periods (results were not sensitive to the precise location chosen). For each period, high heat flux events were defined as the times that Q_{THF} exceeded the 95th percentile value based on these time series (470 W/m^2 for the early winter period and 570 W/m^2 for the midwinter period). If Q_{THF} exceeded this threshold for more than 3 h, the time of the maximum in Q_{THF} was selected to be the time for that particular event. Using this approach, 213 high heat flux events were identified in the early winter period, and 182 events were identified in the midwinter period. Typically, three events occurred each month with each event lasting for about a day on average. Approximately 80% of them were characterized by northwesterly flow.

Composites of the sea level pressure, 10 m wind, air-surface temperature difference (ΔT, defined as the difference between the 2 m air temperature and the skin temperature), and Q_{THF} fields were calculated for the high heat flux events that were characterized by northwesterly flow during both the early and midwinter periods (Figure 3). During both periods, there is an enhanced surface pressure gradient across the convection site—between a deep low to the east of Cape Farewell and high pressure over Labrador—that results in strong northwesterly flow (Figures 3a and 3b). The minimum sea level pressures are approximately 20 mbar lower than the respective climatological means (Figures 2a and 2b), with the midwinter central pressure being 2 mbar deeper than that during the early winter period. Over the region of convection, the peak 10 m wind speeds during both periods were in excess of 15 m/s, with the early winter winds approximately 5% higher than the midwinter winds. The 10 m wind field in the vicinity of the convection site shows evidence of convergent flow originating from air exiting Hudson and Davis Straits.

The composite ΔT field associated with the high heat flux events during both periods (Figures 3c and 3d) is negative, indicating that cold air is flowing over the relatively warm surface waters of the Labrador Sea. This field is more negative during the midwinter period. Given the relatively constant sea surface temperature in the region, this is the result of the colder air temperatures both over and upstream of the Labrador Sea during the midwinter period. To the northwest, the cold shelf waters associated with the Labrador Current contribute to reduced ΔT upstream of the convection site during the early winter period. During the midwinter period, the presence of sea ice along the Labrador Coast acts to further reduce the air-sea temperature difference, leading to an increase in this field's gradient upwind of the convection region.

The composite Q_{THF} field has a similar structure during both periods (Figures 3e and 3f) but has a maximum that is higher by approximately 20% during the midwinter period, compared to the early winter period. Given the similarity of the composite 10 m wind fields during both periods, the increase in magnitude of Q_{THF} is the result of the colder air temperatures during the midwinter period.

4. Discussion

In this paper, the characteristics of the atmospheric forcing over the Labrador Sea oceanic convection region have been investigated. Previous work has largely focused on the middle or late winter period when the convective overturning of the water column is most pronounced [*Marshall et al.*, 1998; *Renfrew and Moore*, 1999; *Renfrew et al.*, 1999; *Pagowski and Moore*, 2001; *Renfrew et al.*, 2002; *Myers and Donnelly*, 2008]. However, the buoyancy loss that occurs earlier in the season plays an important role in reducing the stratification of the water column. To date, there has been little research into the atmospheric forcing during this preconditioning phase. Furthermore, there have been no systematic climatologies of high heat flux events in the region. We have addressed both of these issues by considering the mean climatological conditions, as well as composite high heat flux events, during both the early winter (November and December) and midwinter (January and February) periods. This was done using NARR surface meteorological fields, together with the air-sea heat flux fields derived from them using a bulk formulation that has been validated against heat flux measurements in the region [*Renfrew et al.*, 2002]. The high spatial resolution of the NARR allows it to more completely resolve mesoscale features of the surface meteorology in the region.

Our results have revealed a surprising degree of similarity with respect to the spatial structure of the surface meteorological and air-sea heat flux fields for the mean climatological conditions, as well as for the high heat flux events, during both the early and midwinter periods. In particular, northwesterly flow associated with a low-pressure center to the east of Cape Farewell characterizes the climatological mean conditions during both winter periods (Figures 2a and 2b). This is true as well for the high heat flux events, during which the enhanced winds coincide with the region where convection regularly occurs (Figures 3a and 3b). This suggests that the location and depth of the Icelandic Low, along with its associated surface wind field, play a fundamental role in dictating the convection in the Labrador Sea. Such a notion is consistent with earlier studies that have noted the importance of the North Atlantic Oscillation (NAO) in influencing convection [*Dickson et al.*, 1996; *Pickart et al.*, 2002; *Våge et al.*, 2009a]. However, in contrast to conventional thinking, our results imply that the location of the ice edge is not the key factor for determining where the convection

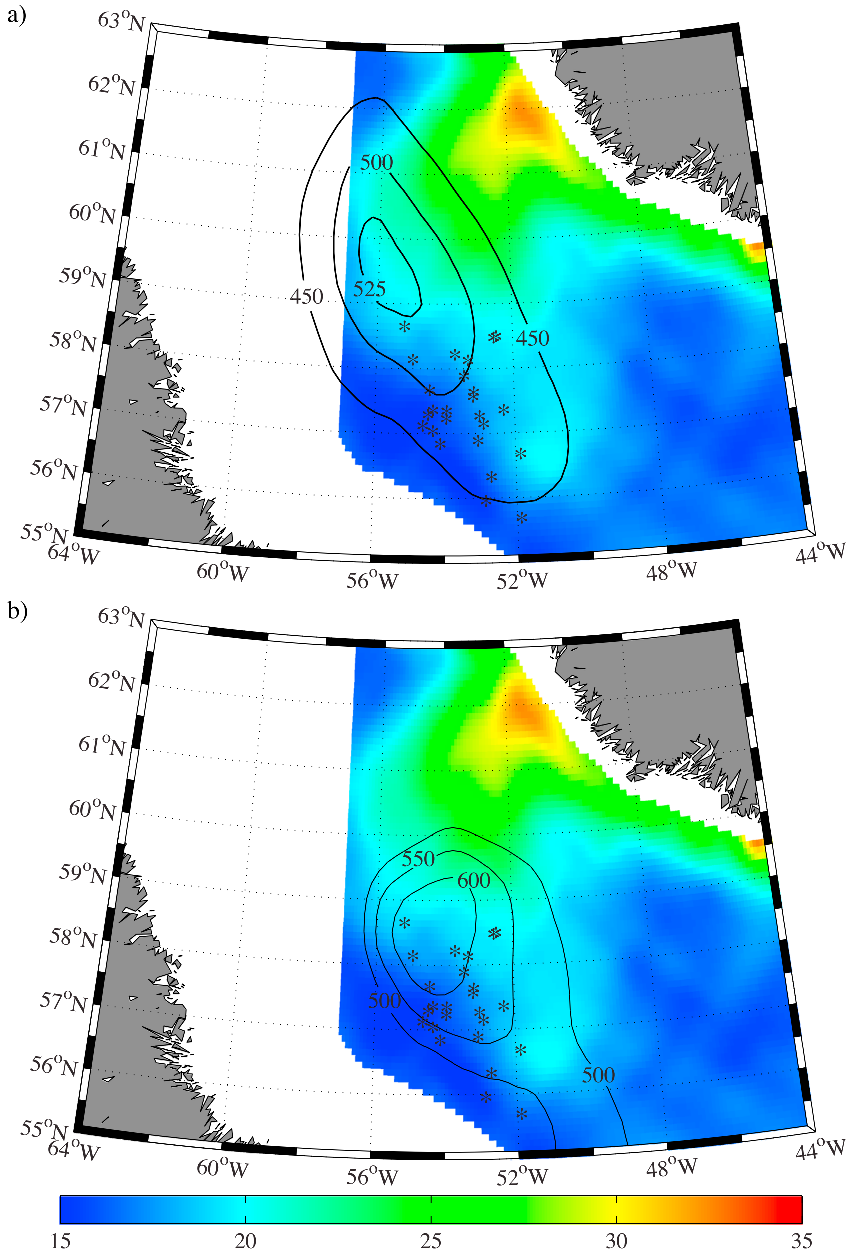

Figure 4. The surface oceanic eddy field (shading: cm s^{-1}, from *Lilly et al.* [2003]) in relation to the composite turbulent heat flux field of Figures 3e and 3f (W m^{-2}: selected contours) during (a) November and December and (b) January and February 1979–2102. The asterisks denote where PALACE floats measured mixed-layer depths exceeding 800 m during the years 1994–1999 [from *Lavender et al.*, 2000].

takes place. Although the ice edge moves considerably southward from the early to late winter period, to first order the region of maximum Q_{THF} remains stationary (Figures 3e and 3f).

Recent work has highlighted the existence of multidecadal mobility in the location of the NAO's northern center of action [*Moore et al.*, 2013; *Raible et al.*, 2013] that, based on the results presented here, may contribute to the variability in the atmospheric forcing of oceanic convection in the region. The flow distortion arising from the interaction of extratropical cyclones with the high topography of Greenland results in a number of wind speed phenomena in the region such as tip jets and barrier flow [*Doyle and Shapiro*, 1999; *Moore*, 2003; *Moore and Renfrew*, 2005; *Renfrew et al.*, 2008]. In the present case, the impact of Greenland on the upstream flow over the Labrador Sea appears to be manifested as an enhanced sea level pressure gradient across the area. This in turn may be related to a decrease in the spacing between the low-pressure systems and the trailing highs that is the result of the reduction in their propagation speed as they interact with Greenland [*Hoskins and Hodges*, 2002; *Våge et al.*, 2009b]. There is also evidence that the high topography in the upwind region associated with the flow of air through Hudson and Davis Straits may affect the location of the heat flux maximum.

Despite the overall similarities in atmospheric forcing between the two time periods considered here, changes in the air-sea fluxes do occur as the cold season progresses that may impact oceanic convection. Based on Profiling Autonomous Lagrangian Circulation Explorer (PALACE) float data and hydrographic data collected prior to the Argo program—during a period of strong convection—the deepest mixed layers tend to occur in the southwest quadrant of the Labrador Sea within the cyclonic recirculation offshore of the boundary current [*Lavender et al.*, 2000; *Pickart et al.*, 2002]. This roughly corresponds to the southern half of the convection region determined from the Argo data (Figures 3e and 3f). It has been argued that this is largely due to the presence of buoyant water that spreads across the northern portion of the basin as a result of anticyclonic eddies generated on the eastern boundary [*Pickart et al.*, 2002; *Lilly et al.*, 2003; *Pickart et al.*, 2008]. In particular, the deepest mixed layers are found southward of the tongue of high oceanic eddy variability emanating from the west Greenland slope (Figure 4).

The earlier studies did not attribute these deeper mixed layers to the spatial pattern of the air-sea heat loss, but rather to the oceanic preconditioning. Our study suggests, however, that the atmosphere may be playing a role as well. Even though the spatial structure of Q_{THF} does not change much between the two composites of Figures 3e and 3f, there is an important difference between the early winter period and the midwinter period. Specifically, the region of maximum heat loss shifts roughly 100 km to the southeast and increases in magnitude (Figure 4). This is primarily the result of the colder surface air temperatures later in the season, which in turn is partly due to the presence of ice over the shelf that minimizes the upstream air mass modification [*Renfrew and Moore*, 1999; *Liu et al.*, 2006]. As such, early in the season, the largest air-sea heat fluxes are located within the tongue of high eddy variability that inhibits oceanic convection, but later in the season, the maximum heat loss is south of the tongue where the deepest mixed layers are observed. This implies that the atmospheric forcing and oceanic preconditioning together dictate where the deepest mixed layers develop.

Due to the primary role of the wind field upstream of the low-pressure systems propagating east of Greenland, the Labrador Sea oceanic convection is similar to that which occurs in the Irminger Sea where the high topography of Greenland is responsible for the high wind speed events that force the overturning [*Pickart et al.*, 2003; *Våge et al.*, 2009b]. In contrast, the other oceanic convection sites in the subpolar North Atlantic occur downstream of the ice edge in the Iceland and Greenland Seas [*Swift et al.*, 1980; *Marshall and Schott*, 1999]. In these regions, there is no obvious topographic contribution to the surface wind field, and so the distribution of pack ice may play the dominant role in determining the spatial distribution of the air-sea heat flux fields.

In a warming climate, with a retreat of sea ice in the Labrador Sea [*Kiilsholm et al.*, 2003], midwinter conditions should be similar to current early winter conditions, i.e., with an ice edge to the north of the convection region. Although our results suggest that this would result in only a modest reduction in the magnitude of the air-sea turbulent heat fluxes, it would nevertheless shift the maximum in the atmospheric forcing northward into the region where eddy activity would inhibit convection. Thus, the processes identified in this paper suggest a weakening of Labrador Sea water formation in a warming climate, a result consistent with recent modeling and observational studies [*Stouffer et al.*, 2006; *Rhein et al.*, 2011; *Robson et al.*, 2014].

Acknowledgments
The authors would like to acknowledge the NOAA Environmental Systems Laboratory for access to the NARR data and the National Snow and Ice Data Center for access to the NASA Team sea ice data. G.W.K.M. was supported by the Natural Sciences and Engineering Research Council of Canada. R.S.P. was supported by grant OCE-085041 from the U.S. National Science Foundation. I. A.R. would like to acknowledge support from NERC grant NE/I005293/1. K.V. received funding from NACLIM, a project of the European Union Seventh Framework Programme under grant agreement 308299.

The Editor thanks two anonymous reviewers for their assistance in evaluating this paper.

References

Brummer, B. (1996), Boundary-layer modification in wintertime cold-air outbreaks from the Arctic sea ice, *Boundary Layer Meteorol.*, *80*(1–2), 109–125.

Clarke, R. A., and J. C. Gascard (1983), The formation of Labrador Sea-Water 1. Large-scale processes, *J. Phys. Oceanogr.*, *13*(10), 1764–1778.

Condron, A., and I. A. Renfrew (2013), The impact of polar mesoscale storms on northeast Atlantic Ocean circulation, *Nat. Geosci.*, *6*(1), 34–37.

DeCosmo, J., K. B. Katsaros, S. D. Smith, R. J. Anderson, W. A. Oost, K. Bumke, and H. Chadwick (1996), Air-sea exchange of water vapor and sensible heat: The humidity exchange over the sea (HEXOS) results, *J. Geophys. Res.*, *101*(C5), 12,001–12,016, doi:10.1029/95JC03796.

Dickson, R., J. Lazier, J. Meincke, P. Rhines, and J. Swift (1996), Long-term coordinated changes in the convective activity of the North Atlantic, *Prog. Oceanogr.*, *38*(3), 241–295.

Doyle, J. D., and M. A. Shapiro (1999), Flow response to large-scale topography: The Greenland tip jet, *Tellus Ser. A*, *51*(5), 728–748.

Fenty, I., and P. Heimbach (2013), Coupled sea ice-ocean-state estimation in the Labrador Sea and Baffin Bay, *J. Phys. Oceanogr.*, *43*(5), 884–904.
Hoskins, B. J., and K. I. Hodges (2002), New perspectives on the Northern Hemisphere winter storm tracks, *J. Atmos. Sci.*, *59*(6), 1041–1061.
Kiilsholm, S., J. H. Christensen, K. Dethloff, and A. Rinke (2003), Net accumulation of the Greenland ice sheet: High resolution modeling of climate changes, *Geophys. Res. Lett.*, *30*(9), 1485, doi:10.1029/2002GL015742.
Kolstad, E. W., et al. (2009), Marine cold-air outbreaks in the North Atlantic: Temporal distribution and associations with large-scale atmospheric circulation, *Clim. Dyn.*, *33*(2–3), 187–197.
Laffineur, T., C. Claud, J. Chaboureau, and G. Noer (2014), Polar lows over the Nordic Seas: Improved representation in ERA-Interim compared to ERA-40 and the impact on downscaled simulations, *Mon. Weather Rev.*, doi:10.1175/MWR-D-13-00171.1.
Lavender, K. L., R. E. Davis, and W. B. Owens (2000), Mid-depth recirculation observed in the interior Labrador and Irminger seas by direct velocity measurements, *Nature*, *407*(6800), 66–69.
Lavender, K. L., R. E. Davis, and W. B. Owens (2002), Observations of open-ocean deep convection in the Labrador Sea from subsurface floats, *J. Phys. Oceanogr.*, *32*(2), 511–526.
Lilly, J. M., P. B. Rhines, F. Schott, K. Lavender, J. Lazier, U. Send, and E. D'Asaro (2003), Observations of the Labrador Sea eddy field, *Prog. Oceanogr.*, *59*(1), 75–176.
Liu, A. Q., G. W. K. Moore, K. Tsuboki, and I. A. Renfrew (2006), The effect of the sea-ice zone on the development of boundary-layer roll clouds during cold air outbreaks, *Boundary Layer Meteorol.*, *118*(3), 557–581.
Marshall, J., and F. Schott (1999), Open-ocean convection: Observations, theory, and models, *Rev. Geophys.*, *37*(1), 1–64, doi:10.1029/98RG02739.
Marshall, J., et al. (1998), The Labrador Sea deep convection experiment, *Bull. Am. Meteorol. Soc.*, *79*(10), 2033–2058.
Mesinger, F., et al. (2006), North American regional reanalysis, *Bull. Am. Meteorol. Soc.*, *87*(3), 343–360.
Moore, G. W. K. (2003), Gale force winds over the Irminger Sea to the east of Cape Farewell, Greenland, *Geophys. Res. Lett.*, *30*(17), 1894, doi:10.1029/2003GL018012.
Moore, G. W. K., and I. A. Renfrew (2005), Tip jets and barrier winds: A QuikSCAT climatology of high wind speed events around Greenland, *J. Clim.*, *18*(18), 3713–3725.
Moore, G. W. K., R. S. Pickart, and I. A. Renfrew (2008), Buoy observations from the windiest location in the world ocean, Cape Farewell, Greenland, *Geophys. Res. Lett.*, *35*, L18802, doi:10.1029/2008GL034845.
Moore, G. W. K., I. A. Renfrew, and R. S. Pickart (2013), Multidecadal mobility of the North Atlantic Oscillation, *J. Clim.*, *26*(8), 2453–2466.
Myers, P. G., and C. Donnelly (2008), Water mass transformation and formation in the Labrador Sea, *J. Clim.*, *21*(7), 1622–1638.
Olsson, P. Q., and J. Y. Harrington (2000), Dynamics and energetics of the cloudy boundary layer in simulations of off-ice flow in the marginal ice zone, *J. Geophys. Res.*, *105*(D9), 11,889–11,899, doi:10.1029/1999JD901194.
Pagowski, M., and G. W. K. Moore (2001), A numerical study of an extreme cold-air outbreak over the Labrador Sea: Sea ice, air-sea interaction, and development of polar lows, *Mon. Weather Rev.*, *129*(1), 47–72.
Parkinson, C. L., and D. J. Cavalieri (2008), Arctic sea ice variability and trends, 1979–2006, *J. Geophys. Res.*, *113*, C07004, doi:10.1029/2007JC004564.
Petersen, G. N., and I. A. Renfrew (2009), Aircraft-based observations of air-sea fluxes over Denmark Strait and the Irminger Sea during high wind speed conditions, *Q. J. R. Meteorol. Soc.*, *135*(645), 2030–2045.
Pickart, R. S., D. J. Torres, and R. A. Clarke (2002), Hydrography of the Labrador Sea during active convection, *J. Phys. Oceanogr.*, *32*(2), 428–457.
Pickart, R. S., M. A. Spall, M. H. Ribergaard, G. W. K. Moore, and R. F. Milliff (2003), Deep convection in the Irminger Sea forced by the Greenland tip jet, *Nature*, *424*(6945), 152–156.
Pickart, R. S., K. Våge, G. W. K. Moore, I. A. Renfrew, M. H. Ribergaard, and H. C. Davies (2008), Convection in the western North Atlantic subpolar gyre: Do small-scale wind events matter?, in *Arctic-Subarctic Ocean Fluxes: Defining the Role of the Northern Seas in Climate*, edited by R. R. Dickson, J. Meincke, and P. Rhines, pp. 629–652 , Springer, Houten, Netherlands.
Raible, C. C., F. Lehner, J. F. Gonzalez Rouco, and L. Fernandez Donado (2013), Changing correlation structures of the Northern Hemisphere atmospheric circulation from 1000 to 2100 AD, *Clim. Past Discuss.*, *9*(4), 4987–5018.
Renfrew, I. A., and G. W. K. Moore (1999), An extreme cold-air outbreak over the Labrador Sea: Roll vortices and air-sea interaction, *Mon. Weather Rev.*, *127*(10), 2379–2394.
Renfrew, I. A., G. W. K. Moore, T. R. Holt, S. W. Chang, and P. Guest (1999), Mesoscale forecasting during a field program: Meteorological support of the Labrador Sea deep convection experiment, *Bull. Am. Meteorol. Soc.*, *80*(4), 605–620.
Renfrew, I. A., G. W. K. Moore, P. S. Guest, and K. Bumke (2002), A comparison of surface layer and surface turbulent flux observations over the Labrador Sea with ECMWF analyses and NCEP reanalyses, *J. Phys. Oceanogr.*, *32*(2), 383–400.
Renfrew, I. A., et al. (2008), The Greenland flow distortion experiment, *Bull. Am. Meteorol. Soc.*, *89*(9), 1307–1324.
Renfrew, I. A., G. N. Petersen, D. A. J. Sproson, G. W. K. Moore, H. Adiwidjaja, S. Zhang, and R. North (2009), A comparison of aircraft-based surface-layer observations over Denmark Strait and the Irminger Sea with meteorological analyses and QuikSCAT winds, *Q. J. R. Meteorol. Soc.*, *135*(645), 2046–2066.
Rhein, M., D. Kieke, S. Hüttl-Kabus, A. Rößler, C. Mertens, R. Meißner, B. Klein, C. W. Böning, and I. Yashayaev (2011), Deep water formation, the subpolar gyre, and the meridional overturning circulation in the subpolar North Atlantic, *Deep Sea Res. Part II*, *58*(17–18), 1819–1832.
Robson, J., D. Hodson, E. Hawkins, and R. Sutton (2014), Atlantic overturning in decline?, *Nat. Geosci.*, *7*(1), 2–3.
Sathiyamoorthy, S., and G. W. K. Moore (2002), Buoyancy flux at ocean weather station Bravo, *J. Phys. Oceanogr.*, *32*(2), 458–474.
Skamarock, W. C. (2004), Evaluating mesoscale NWP models using kinetic energy spectra, *Mon. Weather Rev.*, *132*(12), 3019–3032.
Smith, S. D. (1988), Coefficients for sea-surface wind stress, heat-flux, and wind profiles as a function of wind-speed and temperature, *J. Geophys. Res.*, *93*(C12), 15,467–15,472, doi:10.1029/JC093iC12p15467.
Smith, S. R., D. M. Legler, and K. V. Verzone (2001), Quantifying uncertainties in NCEP reanalyses using high-quality research vessel observations, *J. Clim.*, *14*(20), 4062–4072.
Stouffer, R. J., et al. (2006), Investigating the causes of the response of the thermohaline circulation to past and future climate changes, *J. Clim.*, *19*(8), 1365–1387.
Swift, J. H., K. Aagaard, and S. A. Malmberg (1980), Contribution of the Denmark Strait overflow to the deep North Atlantic, *Deep Sea Res. Part A*, *27*(1), 29–42.
Talley, L. D., J. L. Reid, and P. E. Robbins (2003), Data-based meridional overturning streamfunctions for the global ocean, *J. Clim.*, *16*(19), 3213–3226.
Våge, K., R. S. Pickart, V. Thierry, G. Reverdin, C. M. Lee, B. Petrie, T. A. Agnew, A. Wong, and M. H. Ribergaard (2009a), Surprising return of deep convection to the subpolar North Atlantic Ocean in winter 2007–2008, *Nat. Geosci.*, *2*(1), 67–72.
Våge, K., T. Spengler, H. C. Davies, and R. S. Pickart (2009b), Multi-event analysis of the westerly Greenland tip jet based upon 45 winters in ERA-40, *Q. J. R. Meteorol. Soc.*, *135*(645), 1999–2011.